Structural Features of Twisted Stacked-Tape Cables With High Lorentz Loads Using Finite Element Analysis

Federica Pierro, Zijia Zhao, Luisa Chiesa, and Makoto Takayasu

***Abstract*—Structural support features for a twisted stacked-tape cable (TSTC) were evaluated through finite element analysis (FEA) to evaluate the mechanical performance of a TSTC surrounded with a rigid copper core and exposed to transverse compression. Annealing of the copper core can occur during the manufacturing process; so, the stress accumulation of the stack was studied as a function of yield strength of the copper, and the results suggested that a lower yield strength copper would result in higher stress accumulation in the tape stack. To ensure adequate support for the cable, two possible solutions were presented: increasing the core diameter or adding a stainless-steel jacket outside the core containing the stack of tapes. Both options resulted in similar reduction in the maximum stress of the tapes. The mechanical stability of a conductor can also be affected by the thickness of the tapes used in the cable. For the same cable dimensions, higher current densities can be obtained using thinner tapes, which however could jeopardize the mechanical integrity of the support. Different tape architectures, varying substrate, and copper stabilizer thicknesses were also studied. Results suggested that for the same amount of current carried by each tape, thinner tapes will experience higher stress. Finally, a full-scale twisted model was developed. A more complex and time-consuming twisted model provides results that are very similar to the simpler untwisted configuration used in this work, justifying its utilization.**

***Index Terms*—High-temperature superconductors, superconducting cables, superconducting magnets, electromagnetic forces, transverse compression.**

I. Introduction

FUTURE high field magnets for particle accelerator and fusion machines will need to produce magnetic fields higher than 20 T [1] while operating between 4.2 K and 20 K [2]. As traditional superconducting magnets made with niobium-titanium (NbTi) and niobium-tin (Nb_3Sn) magnets cannot operate at those high magnetic fields, more recent work has been focusing on high temperature superconductors (HTS) and, in particular, second generation (2G) REBCO (rare-earth barium-copper-oxide) tapes to achieve such conditions [3], [4].

F. Pierro, Z. Zhao, and L. Chiesa are with the Mechanical Engineering Department, Tufts University, Medford, MA 02155 USA (e-mail: Federica.Pierro@tufts.edu; Zijia.Zhao@tufts.edu; Luisa.Chiesa@tufts.edu).

M. Takayasu is with the Plasma Science and Fusion Center, MIT, Cambridge, MA 02139 USA (e-mail: takayasu@psfc.mit.edu).

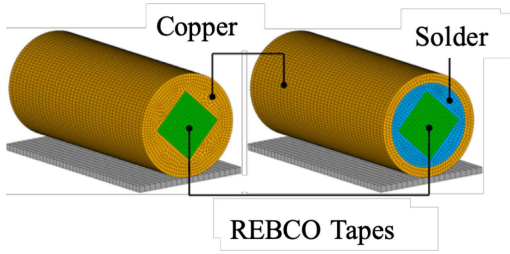

Fig. 1. A 40-tape stacked-tape cable with two supports methods: (a) solid copper core and (b) solder filled tube [12].

Although REBCO tapes exhibit excellent mechanical properties in addition to their higher electromagnetic performance when compared to low temperature superconductors, their flat geometry poses a challenge when fabricating multi-tape cables.

A variety of cable configurations have been developed to address the need for high-current density. These configurations include the Roebel Assembled Coated Conductor (RACC) [5], the Twisted Stacked-Tape Cable (TSTC) [6], the Conductor in Round Core (CORC) [7], and other variations involving multiple tapes [8], [9].

To ensure good performance in high current and high field, it is necessary to account for the natural electromagnetic Lorentz forces that occur in these conditions. These forces, caused by the interaction between the high currents and the high magnetic field, can cause large, accumulating transverse compression in the cable that can degrade its electrical performance [10], [11].

In previous work [12], [13], we started investigating the effect of electromagnetic transverse compressive loads on an untwisted 40-tape TSTC using numerical finite element analysis. Two support methods were modeled: a solid cylindrical hard copper core and a solder filled tube (Fig. 1). The corresponding stress/strain conditions were analyzed in both supporting methods for loads up to 1000 kN/m for different geometrical parameters of the cable (tube thickness, tube diameter, conductor's width, etc.).

In this work, the effect on the stress distribution in the stack for both supporting configurations is investigated as a function of the following parameters: the yield strength of the adopted copper core, the impact of using a stainless-steel jacket on the stress distribution within the stack, and the tape's architecture (substrate and copper stabilizer thicknesses). Finally, a full 200 mm twist pitch cable is modeled for the solid core configuration and the results of the twisted cable are compared with

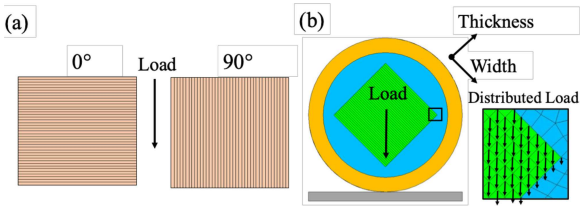

Fig. 2. (a) Stack orientation angles: 0° and 90°. (b) Nodal distribution of the applied electromagnetic Lorentz load for the TSTC solder filled tube model (stack oriented at 45°) and specification of thickness and width directions (defined with respect to the width and thickness of the tape).

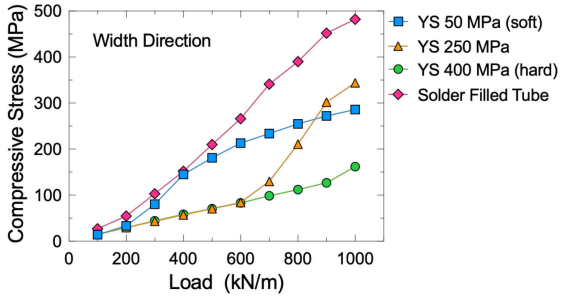

Fig. 3. Plot of the maximum compressive stress in the tape stack as a function of load for the solid core configuration with varying copper core stiffness. Results are compared with stress of the solder filled tube configuration.

the straight cable configuration (used for all the results discussed here) to highlight similarities and differences.

II. Finite Element Model

A full-scale three-dimensional model of a stacked-tape cable under transverse compression was investigated with ANSYS. A 40-tape cable made with 4 mm wide SuperPower REBCO tapes was modeled with two support structures as shown in Fig. 1. The stack is either surrounded by solid copper (Fig. 1 (a)), or enclosed by a copper tube (0.8 mm thick) filled with solder (Fig. 1 (b)). The outside diameter for both configurations is 8.4 mm.

The cable was analyzed in both untwisted and twisted configurations. The twisted model is one full twist pitch of 200 mm in length and the stack of tapes is twisted around its axis, while in the untwisted configuration a stack of tapes oriented at 45 degrees was used. This orientation is the most critical orientation for the tapes when applying an accumulating electromagnetic load, as the tapes experience the highest stress in both width and thickness direction [12]. In the straight configuration, the orientation angle the stack is defined with respect to the Lorentz load: when the compressive load is perpendicular to the wide face of the tape the stack is orientated at 0° (Fig. 2(a)).

A maximum load of 1000 kN/m was applied in both models as a distributed vertical load acting on each tape of the stack (Fig. 2(b)).

HTS tapes were modelled using SOLSH190 structural solid-shell elements, while structural solid element SOLID185 was used for the support structure and the bottom plate. The geometry was meshed with brick elements. Mesh density was defined based on a mesh study conducted in [12] and resulting in an element size of 0.1 mm for the tapes and 0.25 mm for the remaining support structure. Bilinear material properties were used to define the nonlinear deformation occurring in the tapes [12], [13]. Contact pairs (TARGET170 and CONTA174) were used to describe the interaction between neighboring tapes as well as the tapes and the core. A rigid plate was used to support the entire cable and was fixed in all directions. Symmetry-style conditions were prescribed to the ends of the cable. Additional details of the finite element models and material properties of the tape, core and solder were described in [12] and [13].

The aim of the simulations presented in this paper is to provide guidelines for future cable design by investigating the ability of the two support methods to reduce the stress in the stack. The geometry of the two support methods investigated in this work are idealizations of the real structure of the cable (described in [6]). Although details of the geometry were omitted from the simulation in order to simplify the computation, the results shown in this work can be used to identify the stress behavior of the tapes as function of the analyzed parameters. However, due to the simplifications made in the model, absolute stress values in real cables could differ.

The maximum stress shown in the plots of the following sections was found using average elemental stress data in the conductor for 95% of the elements through the cross section of the stack. Results for the remaining 5% of the elements was disregarded to mitigate the effect of localized stress concentration generated by the simulation, as described in [12]. The 95% stress range was proved to be the method that disregard the smallest number of elements while removing singular points generated by the simulations. On the other end, disregarding more than 5% of elements would mean neglecting stress state experienced by a higher number of elements and therefore representative of the stress distribution in the stack.

III. Finite Element Results

In this sections, results of the finite element models are presented for the configurations previously described.

A. Annealed Copper

In previous work [12], [13] it was assumed that the copper surrounding the stack of tapes (for both solid core and solder filled tube configuration) was unprocessed hard copper which has an elastic modulus of 120 GPa and yield stress of 400 MPa [15]. However, copper may experience annealing during the manufacturing process of the core (before inserting the stack), which may result in a softer support material (OFHC could have a yield stress as low as 50 MPa [16]).

To investigate the effect of the yield strength of the copper core, a study was conducted using copper with the elastic modulus of 120 GPa but three different yield stresses (YS): 50 MPa (fully annealed, soft), 250 MPa and 400 MPa (hard). Fig. 3 shows the effect of the yield strength of the copper on the maximum stress of the tapes in the width direction (indicated in Fig. 2 (b)) as a function of load. Fig. 3 shows that for a soft copper core (YS 50 MPa), the stress in the width direction is changing linearly

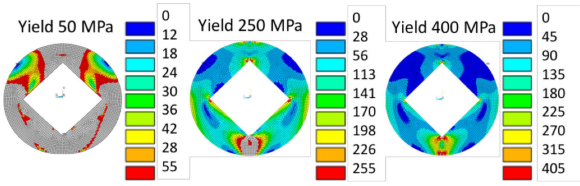

Fig. 4. Contour plot of von Mises stress (MPa) in the copper core at 300 kN/m. The portion of the plot which is not represented by a color in the legend indicates the area plastically deformed, where the stress is higher than the specified yield strength for the copper.

for loads smaller than 300 kN/m. A similar trend is observed for the other cases as well, but at higher loads (700 kN/m for YS 250 MPa and 1000 kN/m for YS 400 MPa). In Fig. 4 contour plots of von Mises stress in the copper cores with different yield strengths are shown at a given load (300 kN/m). For soft copper (YS 50 MPa) the majority of the core experiences a stress higher than its specified yield strength (plastic deformation is occurring). For the same load, the copper remains elastic if its yield strength is 250 MPa or 400 MPa.

From these findings we can conclude that if the stress experienced by the copper support material is greater than its yield strength, the support material plastically deforms and the stress in the stack no longer increases linearly with the load. Moreover, the lower the yield strength of the copper, the lower is the load at which such change occurs.

At 1000 kN/m, the maximum stress in the stack in the width direction is around 300 MPa when using annealed copper core (YS 50 MPa), while it is less than 150 MPa when using hard copper (YS 400 MPa). In Fig. 3 the results are also compared with previous findings for the solder filled tube configuration.

As it can be seen, compared to the fully annealed copper core (YS 50 MPa), the solder filled configuration has a much higher stress in the width direction (most critical for delamination). In this direction, a fully annealed copper core (YS 50 MPa) results in a stress reduction of 40% compared to the solder filled tube.

In the thickness direction, the stress increased linearly through the entire range of loads (up to 1000 kN/m) with the soft copper experiencing the largest stresses.

If it is hard to avoid annealing of the copper core during the manufacturing process, two potential solutions to improve the support of the stack might be utilized: increasing the core diameter or adding a stainless-steel jacket outside of the cable.

B. Copper Core Diameter and Stainless Steel Jacket

To minimize the stress accumulation in the tapes when using a fully annealed copper (YS 50 MPa), the core diameter was increased to the following values: 8.9 mm, 9.4 mm, and 9.9 mm. Fig. 5 shows the effect of the yield stress of the copper on the maximum stress values as a function of load in the width direction of the tape. At the maximum load of 1000 kN/m the stress in the width direction is 31% smaller with a 9.9 mm diameter compared to the original 8.4 mm diameter with soft copper. However, the stress is still 21% higher than the 8.4 mm diameter using hard copper. A similar behavior was observed in the thickness direction (stress being 42% lower with a 9.9 mm diameter

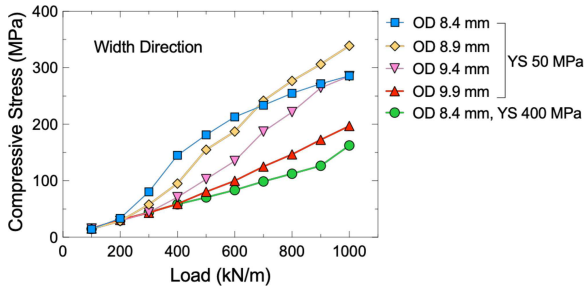

Fig. 5. Plot of the maximum compressive stress in the tape stack as a function of load for the solid core configuration with soft copper (YS 50 MPa) and different core diameters. Hard copper with nominal 8.4 mm diameter is also shown for comparison.

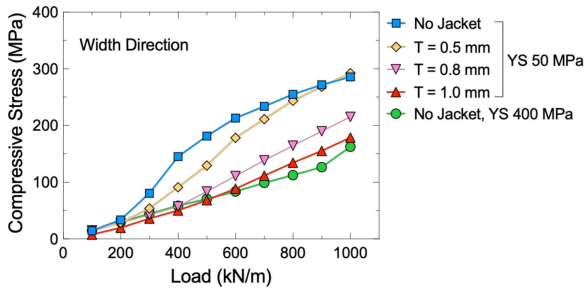

Fig. 6. Plot of the maximum compressive stress in the tape stack as a function of load for the solid core configuration with stainless steel jacket of various thicknesses compared to cases without a jacket (soft and hard copper).

compared to the original 8.4 mm). In addition, the larger is the diameter of the core, the lower is the fraction of the core that plastically deforms at a given load so that the nonlinear increase of the stress discussed in Fig. 3 will occur at higher loads.

Another alternative to reduce the stress accumulation in the tapes is to include an external stainless steel jacket (316LN material properties listed in [17]) of various thicknesses (0.5 mm, 0.8 mm, and 1 mm). Similarly to increasing the copper core diameter, a reduction on the maximum stress experienced by the stack is observed when the stainless steel jacket is utilized (See Fig. 6 for results in the width direction).

In particular, when using a 1 mm thick jacket, the stress in the width direction is comparable to the case with 400 MPa yield stress hard copper. The stress in the thickness direction showed a similar behavior.

C. Tape Architecture

In recent years interest towards REBCO tapes made with thinner substrate (compared to the conventional $\sim$50 μm) and copper stabilizer has been increasing. Among the advantages of thinner tapes are the possibility of achieving higher current density and higher cable's bendability [18], [19]. On the other end, a reduction of the thickness of the Hastelloy substrate will results in a weaker mechanical support against Lorentz load and may cause higher strain and larger current degradation on each individual tape. In this section, we investigated the effect of Lorentz Load on a stack containing tapes with 30 μm substrate and 10 μm or 40 μm copper stabilizer. Mechanical properties for the tapes are listed in [20]. Results were compared with finding for the 50 μm

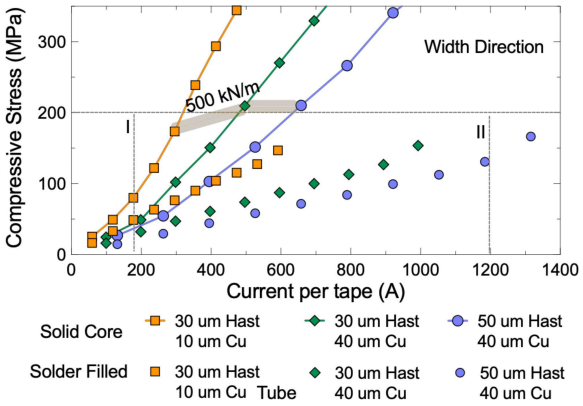

Fig. 7. Plot of the maximum compressive stress (95% of elements) in the tape stack as a function of the current for each tape in the width direction. The stress is represented for a stack oriented at 45 degrees. Current per tape is calculated by dividing the applied load by the number of tapes and the magnetic field (19 T). Two regions are defined by a horizontal stress limit of 200 MPa, and two vertical lines which corresponds to the current carrying capability of the tape in a perpendicular and parallel (to *ab* plane of the tape) background field.

tape. The number of tapes in the stack was modified with the thickness of the tape to maintain a square cross section of the TSTC, while the outer diameter of the copper was kept at 8.4 mm.

The stress in each of the three tape architectures was similar in both width and thickness directions. A similar behavior was observed for the solder filled case. A maximum compressive stress of 200 MPa (dotted horizontal line), is used as the reference for the design of the new generation of magnets [21]. Region I and II are vertically delimited by a current of 180 A and 1200 A, which correspond to the current limit of REBCO at 19 T for a perpendicular and parallel field respectively (current density of 0.45 kA/mm^2 and 3 kA/mm^2) [22].

As Fig. 7 shows, a cable made with a solder filled tube support might sustain Lorentz loads lower than 500 kN/m, as higher loads will result in stresses higher than 200 MPa. For the same amount of current, tapes made with 30 μm substrate and 10 μm copper will experience a higher stress compared to the other two cases (30 μm substrate /40 μm copper and 50 μm substrate/40 μm copper).

The solid core would not be limited by the design constraint of stresses lower than 200 MPa, as the stress is below this threshold even at the maximum load of 1000 kN.

D. Twisted Stack Model

In all the above simulations, the tape-stack has always been represented in the straight untwisted configuration (tapes not twisted along the axis), while orienting the stacked tapes at different angles to replicate the condition of a twisted cable. This approach was used to simplify the computation time, as modeling a full twist pitch cable can be challenging due to the increase mesh density and number of contact elements (2.5 hours for a straight model vs 40 hours for a twisted model). It was assumed that the straight model (in the different orientation angles), would represent a conservative approach to the problem as the stress was expected to be similar or higher compared to the one in the twisted configuration. In order to verify this assumption and

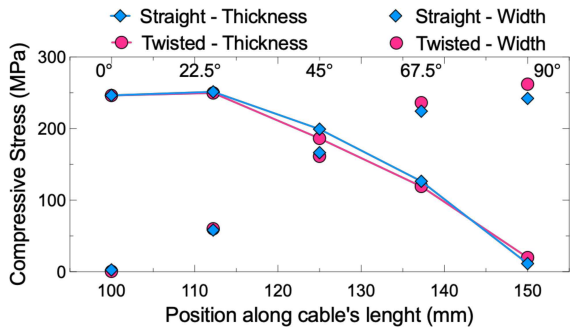

Fig. 8. Plot of the maximum compressive stress in the tape stack along the cable's length (and corresponding orientation angle) for both straight and twisted model (width and thickness directions).

highlight the difference between twisted and straight configuration, a full-scale, 40-tapes, twisted stack model with twist pitch of 200 mm was modeled using a solid core (hard copper, 400 MPa) as support method. The modelled tapes are 4 mm wide, a 50 μm substrate and a 40 μm copper stabilizer. To properly compare the two models, element size, mesh density, loading and boundary conditions were maintained the same.

Fig. 8 shows the comparison between twisted and straight models. The stress values at the orientation angles of 90, 67.5, 45, 22,5 and 0 degree were considered for the straight model. In the twisted configuration, those angles are located in the middle section of the cable (position along a 200 mm long cable between 100 mm and 150 mm), to avoid stress accumulation caused by the end conditions.

As shown in Fig. 8, the stress values obtained in the twisted model are similar to what observed in the straight model for the five orientations investigated. The results obtained suggest that the straight cable model represents reasonably well the stress behavior of a twisted cable while saving time required for the computation.

IV. Conclusion

A finite element method was used to investigate the impact of different cable parameters (material properties, tape architecture, addition of a stainless steel jacketing) on the maximum stress experienced by a stack of tapes in a TSTC. It was found that using a soft copper core (instead of hard copper) results in higher stress in the cable. Increasing the core diameter, as well as including a 1 mm thick stainless steel tube, could reduce this effect. Tapes with different substrate and copper stabilizer thicknesses were also investigated, showing how thinner tapes experience higher stress while carrying the same amount of current compared to thicker tapes. Finally, a fully twisted 200 mm twist pitch cable was modelled, and the results were compared to the corresponding orientation angles in a straight configuration. The results show that the straight model and fully twisted model agree reasonably well, and the straight model can be used to describe the stress in the cable while maintaining a lower computational time.

In future work, the normalized critical current for the cable will be estimated for different orientation angles of the stack for both solid core and solder filled tube configuration.

REFERENCES

[1] L. Rossi *et al.*, "The EuCARD-2 future magnets european collaboration for accelerator-quality HTS magnets," *IEEE Trans. Appl. Supercond.*, vol. 25, no. 3, pp. 1–7, Jun. 2015, Art. no. 4001007.

[2] G. Janeschitz *et al.*, "High temperature superconductors for future fusion magnet systems–status, prospects and challenges," in *Proc. 21st Int. At. Energy Agency Fusion Eng. Conf.*, 2006, vol. 16, no. 21, pp. 10–2006: Citeseer.

[3] G. A. Kirby *et al.*, "Accelerator-quality HTS dipole magnet demonstrator designs for the EuCARD-2 5-T 40-mm clear aperture magnet," *IEEE Trans. Appl. Supercond.*, vol. 25, no. 3, Jun. 2015, Art. no. 4000805.

[4] B. N. Sorbom, *et al.*, "ARC: A compact, high-field, fusion nuclear science facility and demonstration power plant with demountable magnets," *Fusion Eng. Des.*, vol. 100, pp. 378–405, Nov. 2015.

[5] W. Goldacker *et al.*, "Roebel cables from REBCO coated conductors: A one-century-old concept for the superconductivity of the future," *Supercond. Sci. Technol.*, vol. 27, no. 9, Aug. 2014, Art. no. 093001.

[6] M. Takayasu, L. Chiesa, N. C. Allen, and J. Minervini, "Present status and recent developments of the twisted stacked-tape cable conductor," *IEEE Trans. Appl. Supercond.*, vol. 26, no. 2, Mar. 2016, Art. no. 6400210.

[7] D. C. Van der Laan *et al.*, "Characterization of a high-temperature superconducting conductor on round core cables in magnetic fields up to 20 T," *Supercond. Sci. Technol.*, vol. 26, no. 4, Feb. 2013, Art. no. 045005.

[8] G. Celentano *et al.*, "Design of an industrially feasible twisted-stack HTS cable-in-conduit conductor for fusion application," *IEEE Trans. Appl. Supercond.*, vol. 24, no. 3, Jun. 2014, Art. no. 4601805.

[9] N. Bykovsky *et al.*, "Performance evolution of 60 kA HTS cable prototypes in the EDIPO test facility," *Supercond. Sci. Technol.*, vol 29, no. 8, Jun. 2016, Art. no. 084002.

[10] C. Barth *et al.*, "Temperature-and field dependent characterization of a twisted stacked-tape cable," *Supercond. Sci. Technol.*, vol. 28, no. 4, Feb. 2015, Art. no. 045015.

[11] S. Otten *et al.*, "Enhancement of the transverse stress tolerance of REBCO Roebel cables by epoxy impregnation," *Supercond. Sci. Technol.*, vol. 28, no. 6, Apr. 2015, Art. no. 065014.

[12] N. C. Allen, F. Pierro, Z. Zhao, L. Chiesa, and M. Takayasu, "Structural finite element evaluation of twisted stacked-tape cables for high-field magnets," *IEEE Trans. Appl. Supercond.*, vol. 27, no. 4, Jun. 2017, Art. no. 6900205.

[13] F. Pierro *et al.*, "Finite element investigation of the mechanical behaviour of a twisted stacked-tape cable exposed to large lorentz loads," *IOP Conf. Ser.: Mater. Sci. Eng.*, vol. 279, no. 1, 2017, Art. no. 012035.

[14] C. Barth, G. Mondonico, and C. Senatore, "Electro-mechanical properties of REBCO coated conductors from various industrial manufacturers at 77 K, self-field and 4.2 K, 19 T," *Supercond. Sci. Technol.*, vol. 28, no. 4, Feb. 2015, Art. no. 045011.

[15] R. Reed *et al.*, *Low Temperature Mechanical Properties of Copper and Selected Copper Alloys*. Gaithersburg, MD, USA: National Bureau of Standards, 1967.

[16] *Oxygen-free high conductivity Copper, Soft, UNS C10200*, Matweb—Material Property Data Website, Feb. 2019. [On- line]. Available: http://www.matweb.com/search/DataSheet.aspx?MatGUID=a629b7c5-643b44bfb25b9bba7f8140ab

[17] J. Sas, K. P. Weiss, and A. Jung, "The mechanical and material properties of 316LN austenitic stainless steel for the fusion application in cryogenic temperatures," *IOP Conf. Ser.: Mater. Sci. Eng.*, vol. 102, no. 1, 2015, Art. no. 012003.

[18] K. Soumen *et al.*, "Symmetric tape round REBCO wire with J e (4.2 K, 15 T) beyond 450 A mm− 2 at 15 mm bend radius: a viable candidate for future compact accelerator magnet applications," *Supercond. Sci. Technol.*, vol. 31, no. 4, Mar. 2018, Art. no. 059601.

[19] T. Mulder *et al.*, "Development of ReBCO-CORC wires with current densities of 400–600 A/mm 2 at 10 T and 4.2 K," *IEEE Trans. Appl. Supercond.*, vol. 28, no. 3 Apr. 2018, Art. no. 4800504.

[20] Y. Zhang *et al.*, Mechanical and electromechanical property study of 2G HTS wires made on 30 μm thick Hastelloy substrate, Feb. 2019. [Online] Available: http://www.superpower-inc.com/system/files/5MOr1A-05+Zhang.pdf

[21] D. Tommasini *et al.*, Baseline specifications and assumptions for accelerator magnet: Mileston M5.2, Feb. 2019. [Online] Available: http://cds.cern.ch/record/2150689

[22] *Engineering Critical Current Density vs. Applied Field*, National High Magnetic Field Laboratory, Feb. 2019. [Online] Available: https://nationalmaglab.org/magnet-development/applied-superconductivity-center/plots